IJBPAS, March, Special Issue, 2025, 14(3): 53-66

ISSN: 2277–4998

International Journal of Biology, Pharmacy and Allied Sciences (IJBPAS)

'A Bridge Between Laboratory and Reader'

www.ijbpas.com

MOLECULAR DOCKING AND ADMET STUDY OF SELECTIVE PHYTOCHEMICALS AND SYNTHETIC DRUGS AGAINST RESPIRATORY SYNCYTIAL VIRUS, 7LVW FUSION PROTEIN

WAGH H*, GIRBANE V[1], DUPADE D[2], BHOSALE A[4], AND BORAWAKE D[5]

Department of Pharmaceutical Chemistry, TMV's Lokmanya Tilak Institute of Pharmaceutical Sciences, Pune, India: 411037

***Corresponding Author: Mrs. Hrutuja Wagh; E Mail: hrutuja3196@gmail.com**

Received 15th Dec. 2024; Revised 20th Dec. 2024; Accepted 1st Jan. 2025; Available online 15th March 2025

https://doi.org/10.31032/IJBPAS/2025/14.3.1006

ABSTRACT

Respiratory Syncytial Virus (RSV) is a viral infection that predominantly affects the respiratory airways, being more common in younger children and some adults. Despite ribavirin being a commonly used treatment for Respiratory Syncytial Virus, many new and more effective drugs are currently under development. Additionally, computational tools, particularly those used in structure-based drug design, have transformed the drug discovery process. The fusion core of the RSV structure is critical for its ability to fuse, enter, and replicate within host cells. This study aimed to investigate molecular docking and ADMET (Absorption, Distribution, Metabolism, Excretion, and Toxicity) properties of various phytochemicals, which have demonstrated high potential against the RSV virus. The main objective of the research was to highlight phytochemicals, in comparison to synthetic drugs currently available for RSV treatment, show greater potency and essential activity. The 7LVW protein was docked with 50 ligands, with 10 of these ligands producing promising results against RSV. The ligands showed higher docking scores than synthetic drugs, which suggests that these phytochemicals may be suitable for prophylactic treatment against RSV. Among the compounds, Chebulic Acid (-6.27), Hesperidin (-5.57), and Rosmarinic Acid (-6.57) displayed superior docking scores compared to Sisunatovir and Ribavirin. This further indicates that these natural compounds may be more effective alternatives in the treatment of RSV infections.

Keywords: Respiratory Syncytial Virus, Molecular Docking, Phytochemicals, ADMET Analysis, Chebulic Acid, Antiviral Discovery

INTRODUCTION

Respiratory Syncytial Virus (RSV) was first identified in 1956, though it was not initially associated with infections in infants. Morris and his team isolated a new virus from chimpanzees, which they called Chimpanzee Coryza Agent (CCA). Later on, Chanock and his collaborators confirmed that this virus caused respiratory illnesses in humans. It was discovered that many children had antibodies specifically neutralizing CCA, leading to the virus being renamed as Respiratory Syncytial Virus (RSV) **[1]**. In adults, the risk of serious RSV-related illness increases due to chronic lung conditions, circulatory diseases, functional impairments, and higher viral loads. RSV is also a major concern in hospitals, where it poses a significant threat to young infants and those with compromised immune systems. Patients who have undergone bone marrow or lung transplants and contract RSV often face higher mortality rates. The virus belongs to the Orthopneumovirus genus, part of the pneumoviridae family, and is categorized under the order Mononegavirales. RSV is divided into two primary antigenic groups, known as RSV-A and RSV-B, which arise from antigenic drift, duplications in the RSV-G gene, and genome-wide variations, including changes in the RSV-F gene **[2]**.

Structure of respiratory syncytial virus

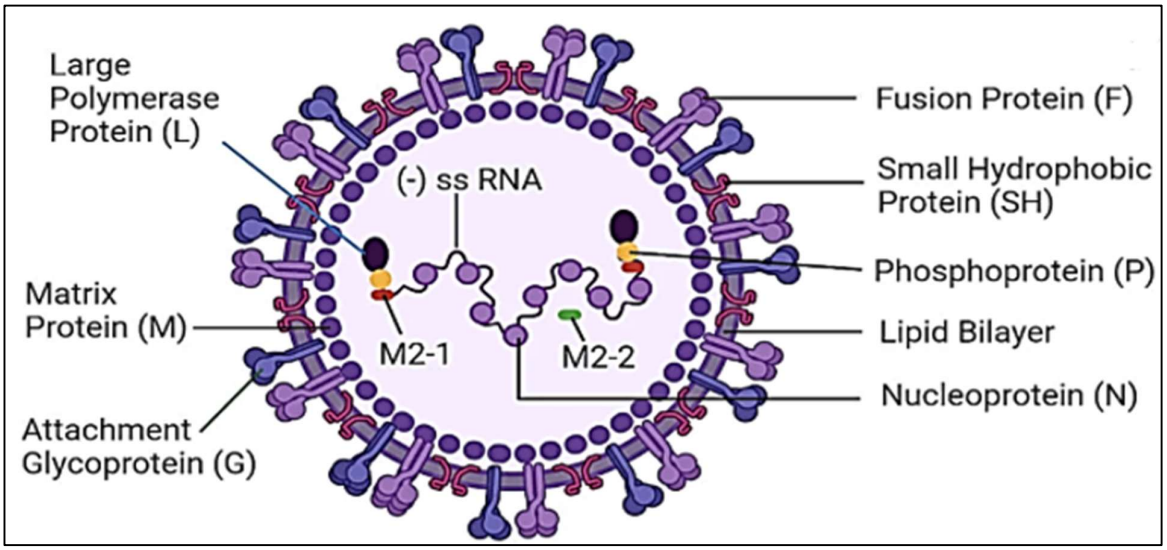

Figure 1: Structure of Respiratory Syncytial Virus

- The RSV virion is comprised of a nucleocapsid encased in a bilipid-layer envelope derived from the host cell membrane.
- When grown in cell cultures, the virion presents as elongated filaments up to 10 µm long and as spherical particles with diameters ranging from 100 to 350 nm.
- The viral envelope is composed of three proteins: the attachment protein (G), the small hydrophobic protein (SH), and the fusion protein (F).

- Viral glycoproteins form individual homo-oligomers that manifest as short surface spikes, measuring between 11 and 16 nm.
- Positioned beneath the lipid membrane is the matrix protein (M).
- The nucleoprotein (N) surrounds a single-stranded, negative-sense RNA, which constitutes the viral genome.
- Associated with the nucleocapsid are the transcription processivity factor M2-1, the phosphoprotein (P), and the RNA polymerase protein (L).

Symptoms of respiratory syncytial virus

Signs and symptoms typically begin five to six days after exposure to RSV and may include:

- Nasal congestion or a runny nose: This is often one of the first signs, making it difficult for the affected individual to breathe comfortably through the nose.
- Dry cough: A persistent cough that does not produce mucus is common and can be bothersome, often worsening at night.
- Mild fever: A slight increase in body temperature can occur, indicating the body's response to the viral infection.
- Sore throat: Irritation or pain in the throat can accompany the infection, contributing to discomfort and difficulty swallowing.
- Frequent sneezing: This reflex action helps to clear the nasal passages but can also be a sign of irritation caused by the virus.
- Headache: Generalized pain or pressure in the head may accompany other symptoms, adding to the feeling of illness.

In more severe cases, symptoms may escalate to:

- High fever: A significant rise in body temperature, which can be higher than 101.3°F (38.5°C), may occur and is a sign of a more intense infection.
- Intense coughing: Severe and persistent coughing can lead to difficulty breathing and may be accompanied by a wheezing sound.
- Wheezing: This high-pitched whistling sound during breathing indicates narrowing of the airways and can be a sign of severe respiratory distress.
- Rapid breathing: An increased rate of breathing, known as tachypnea, can occur as the body tries to get more oxygen due to impaired lung function.
- Bluish discoloration of the skin (cyanosis): This occurs when there is insufficient oxygen in the blood, resulting in a bluish or purplish hue on the skin, particularly around the lips, face, or extremities **[3]**.

Epidemology of respiratory syncytial virus:

Respiratory syncytial virus can be particularly dangerous for several high-risk groups. The elderly, with their often weakened immune

systems, are at an increased risk of severe complications from the virus. Newborns, especially those born prematurely, are highly vulnerable due to their underdeveloped immune and respiratory systems. Individuals with compromised immune systems, including those undergoing treatments that affect their immunity, are also more susceptible to severe RSV infections. Additionally, small children who have pre-existing lung or heart conditions face a higher risk of serious outcomes from RSV. Very young infants, regardless of other health issues, are generally more prone to the severe effects of RSV **[4]**.

MATERIAL AND METHODS

MATERIALS

The 7LVW protein structure was obtained from the Protein Data Bank. Molecular docking and ADMET analyses were conducted using Schrödinger Suite, including Maestro, Glide, and ADMET 2.0. A library of 50 phytochemicals from the IBES database was docked using Glide (HTVS, SP, and EP). Induced-Fit Docking (IFD) was used to refine receptor-ligand interactions. ADMET predictions were made to assess physicochemical properties and toxicity, following Lipinski's Rule of Five.

METHOD

A. Docking Analysis

1. Preparation of protein crystal structure:

The X-ray crystallography process plays a crucial role in determining the detailed atomic structure of proteins, which helps in understanding their functions and interactions with other molecules. The data obtained from this method, when processed correctly, provides insights into how proteins like 7LVW, retrieved from the Protein Data Bank (PDB), can be prepared for computational analysis. In the context of molecular docking studies, this data is refined to ensure accuracy. The X-ray crystallographic structure of 7LVW, available from the Protein Data Bank, was accessed via the DOI link https://doi.org/10.2210/pdb7LVW/pdb.

The Glide software's protein preparation wizard, part of the Schrodinger suite, was employed to correct specific errors in the protein structure, such as missing hydrogen atoms resulting from the X-ray crystallography process. The protocol followed in this study had been previously documented. Bond orders were assigned, and any missing hydrogen atoms within the PDB structure were added as necessary. Additionally, a disulfide bond was formed between sulfur atoms in close proximity, while other settings were kept at their default values. For final refinement, full energetic optimization was conducted using the OPLS3 force field, with the Root Mean Square

Deviation (RMSD) of heavy atoms set at 0.3 Å **[5]** .

2. **Preparation of library of natural compounds**

Approximately 50 naturally derived compounds were sourced from the IBES databases and subsequently uploaded to the Maestro molecular interface (11V5) within the Schrodinger suite workspace. For each 2D structure, low-energy 3D conformers were generated, ensuring that bond lengths and angles were satisfactory. The possible ionization states of each ligand were determined at a physiological pH of 7.2±0.2. All other settings were left at their default values, and the ligands were minimized using the OPLS3 force field. The Ramachandran plot for 7LVW is depicted in **Figure 2 [6]**.

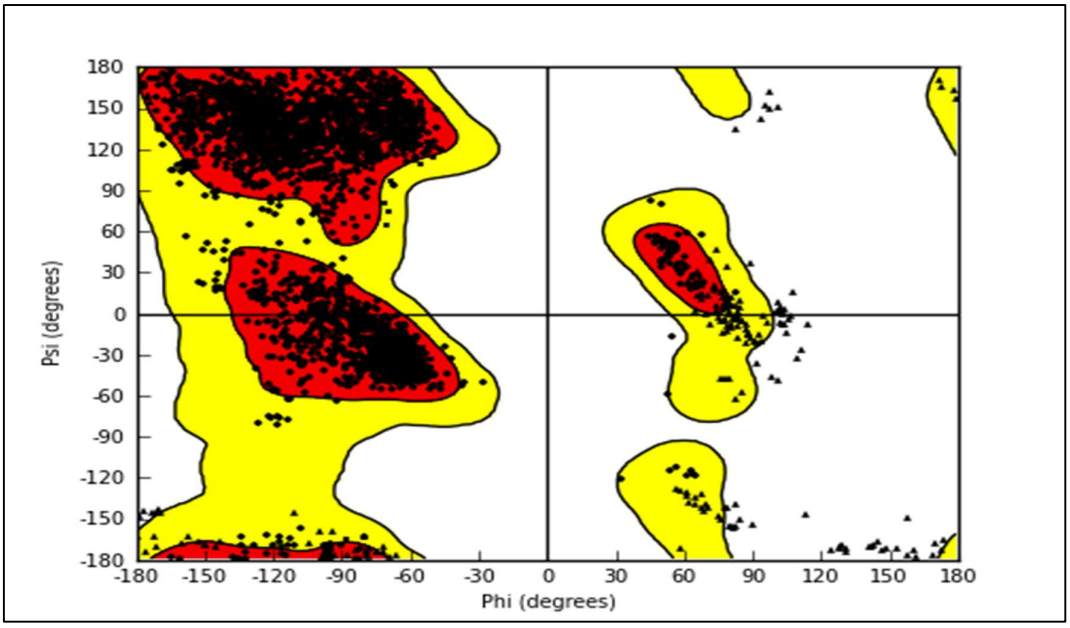

Figure 2: Ramchandran Plot of 7LVW

3. **Site Map and Grid Generation**

The process of sitemap calculation begins with the identification of the site, which is characterized by a set of site points on the grid that are either contiguous or connected by small gaps within solvent-exposed regions. In the subsequent stage, various "maps" are generated to define these sites. Each map represents a set of property values on a 3D grid. For every site, five types of maps—hydrophilic, hydrophobic, donor, acceptor, and surface—are produced and saved as files (.grd files and .vis files). These files can be utilized by Maestro to visualize the surfaces. A total of 12 site maps were created, with the 11th site map scoring -1.39, the highest score among all maps generated Additionally, a grid was created for this site map. The site score of 1.39 indicates that it is particularly promising **[7]**.

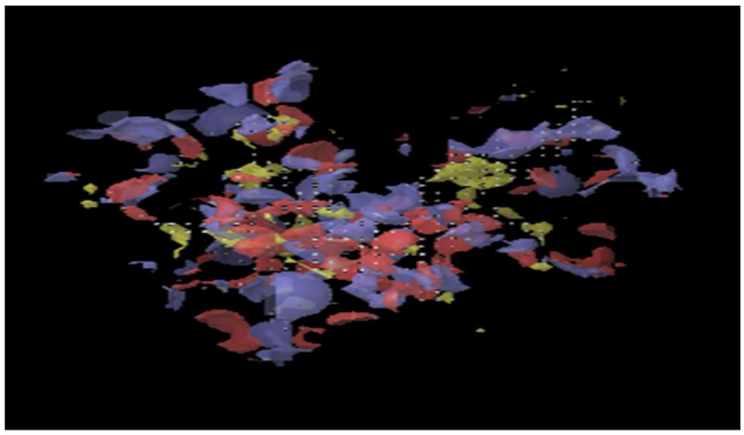

Figure 3: Site Map and Grid Generation of 7LVW

4. Molecular Docking Studies

The Glide grid file was created by using the receptor grid generation panel, selecting the co-crystallized ligand at the protein's active site to automatically determine the x, y, and z coordinates. Glide calculates the default center and size of the grid region based on the ligand's position and dimensions. To screen the 50 compounds, a hierarchical approach using Glide docking was employed, consisting of three stages: High Throughput Virtual Screening (HTVS), Standard Precision (SP), and Extra Precision (EP). HTVS is used for quickly evaluating a large number of ligands with less detailed conformational sampling compared to SP docking. SP docking is suitable for assessing a large number of ligands with unknown properties. EP docking offers a more precise and thorough evaluation but takes longer to complete, making it suitable for high-scoring poses identified in SP docking. The initial screening was performed with SP docking, and the top 30% of poses were then subjected to EP docking for a more refined assessment of binding affinities. To improve the prediction of binding interactions for new inhibitors, Induced-Fit Docking (IFD) was utilized. This protocol aims to enhance docking accuracy by considering potential receptor adjustments in response to the ligand. The process starts with constraint minimization of the receptor, followed by preliminary docking of the ligand using a softened potential. Selected docked poses are then refined with Prime, which includes chain prediction and minimization. Finally, the optimized receptor structures are used for a re-docking process with Glide to assess the ligand binding more accurately **[8]**.

Table 1: Docking, post docking analysis and Binding Free energy of Compounds with 7LVW [11]

Sr. No	Ligand name	IUPAC name	Structure
1	Chebulagic acid	2-[13,14,15,18,19,20,31,35,36-nonahydroxy-2,10,23,28,32-pentaoxo-5-(3,4,5-trihydroxybenzoyl)oxy-3,6,9,24,27,33-hexaoxaheptacyclo[28.7.1.$0^{4,25}$.$0^{7,26}$.$0^{11,16}$.$0^{17,22}$.$0^{34,38}$]octatriacont-1(37),11,13,15,17,19,21,34(38),35-nonaen-29-yl]acetic acid	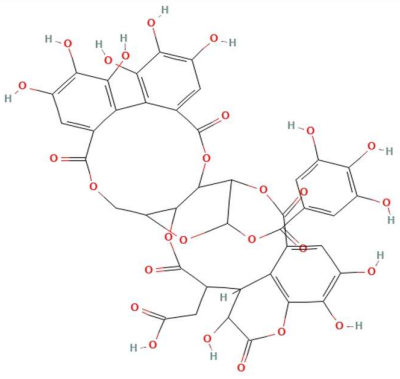
2	Chebulic acid	(2*S*)-2-[(3*S*,4*S*)-3-carboxy-5,6,7-trihydroxy-1-oxo-3,4 dihydroisochromen-4 yl]butanedioic acid	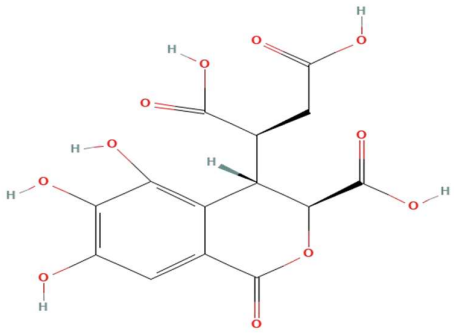
3	Eugenin	5-hydroxy-7-methoxy-2-methylchromen-4-one	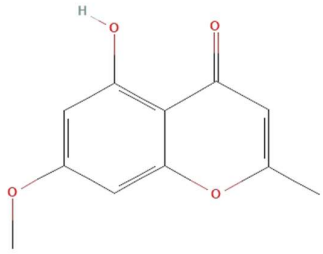
4	Gaultherin	methyl 2-[(2*S*,3*R*,4*S*,5*S*,6*R*)-3,4,5-trihydroxy-6-[[(2*S*,3*R*,4*S*,5*R*)-3,4,5-trihydroxyoxan-2-yl]oxymethyl]oxan-2-yl]oxybenzoate	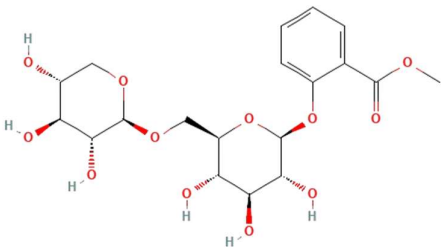

5	**Hesperidin**	**(2*S*)-5-hydroxy-2-(3-hydroxy-4-methoxyphenyl)-7-[(2*S*,3*R*,4*S*,5*S*,6*R*)-3,4,5-trihydroxy-6-[[(2*R*,3*R*,4*R*,5*R*,6*S*)-3,4,5-trihydroxy-6-methyloxan-2-yl]oxymethyl]oxan-2-yl]oxy-2,3-dihydrochromen-4-one**	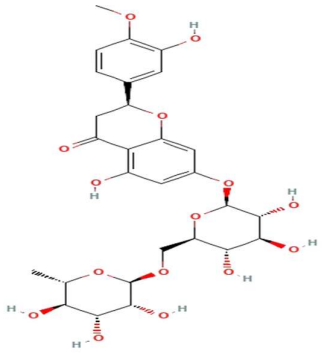
6	**Punarnavoside**	**(2S,3R,5R,9R,10R,13R,14S,17S)-17-[(2R,3R)-2,3-dihydroxy-6-methylheptan-2-yl]-2,14-dihydroxy-10,13-dimethyl-3-[(2R,3R,4S,5S,6R)-3,4,5-trihydroxy-6-(hydroxymethyl)oxan-2-yl]oxy-2,3,4,5,9,11,12,15,16,17-decahydro-1H-cyclopenta[a]phenanthren-6-one**	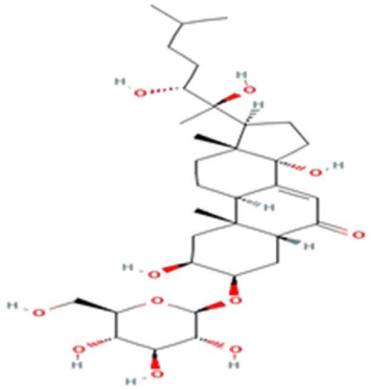
7	**Quercetin**	**2-(3,4-dihydroxyphenyl)-3,5,7-trihydroxychromen-4-one**	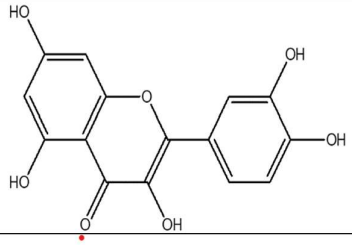
8	**Ribavirin (standard)**	**1-[(2R,3R,4S,5R)-3,4-dihydroxy-5-(hydroxymethyl)oxolan-2-yl]-1,2,4-triazole-3-carboxamide**	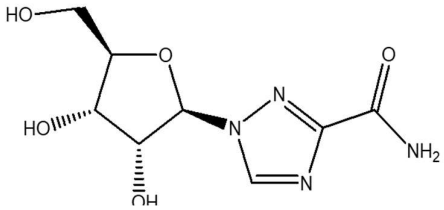
9	**Sisunatovir (Standard)**	**1'-[[5-(aminomethyl)-1-(4,4,4-trifluorobutyl)benzimidazol-2-yl]methyl]-6'-fluorospiro[cyclopropane-1,3'-indole]-2'-one**	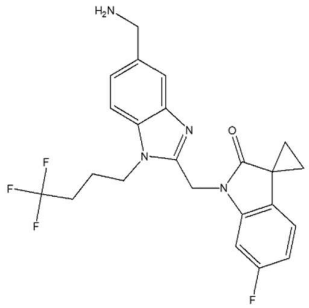

Table 2: Docking, post docking analysis and Binding Free energy of Compounds with 7LVW [11]

Ligands	Docking Score	Binding Free Energy	Interacting Residues
Chebulagic Acid	-4.192	-63.224	Leu231 ,Glu92, Thr249
Chebulic Acid	-6.273	-63.334	Ser255, Glu92, Thr249, Apg235, Apg229
Eugenin	-4.703	-34.552	Thr249, Tyr250,Arg229,Ser238,
Gaultherin	-4.897	-57.885	Arg 235, Glu92, Thr249
Hesperidin	-5.573	-63.610	Lys87, Asp84, Leu231, Glut92, Arg229
Punarnavoside	-4.909	-33.463	Glu92,Leu31,Asn88,Arg235,Asp84
Quercetin	-5.497	-39.207	Asn88,Thr91, Asn254.
Rosamarinic Acid	-6.57	-46.87	Asn228, Thr249, Arg35, Tyr250,Asn88, Asn254
Sisunatovir (Standard)	-5.181	-35.062	
Ribavirin (Standard)	-4.07	-41.101	Glu92,Lys85,Asp84,Arg235

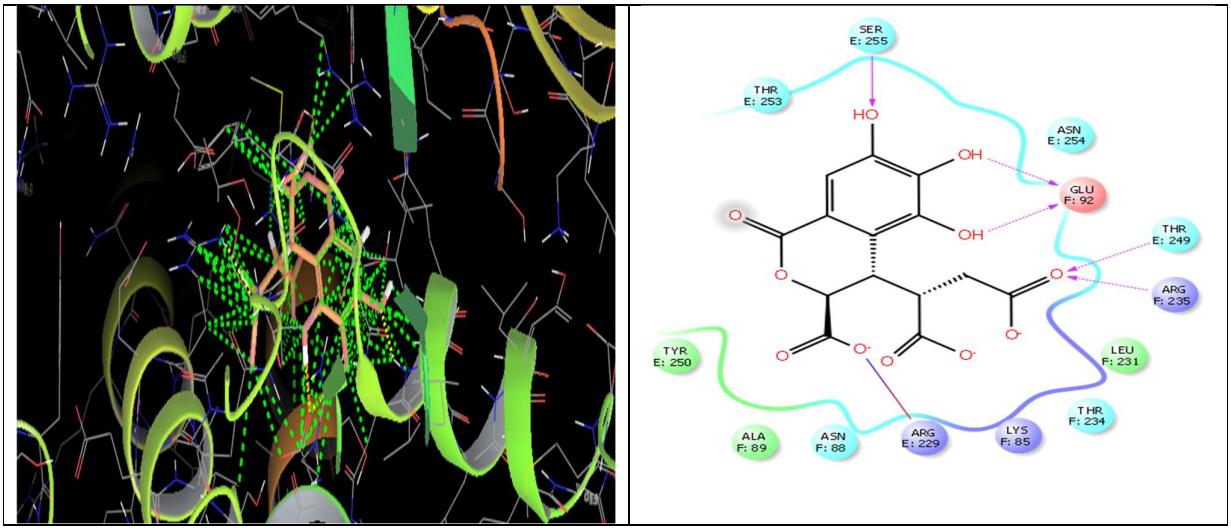

Figure 4: Interaction of Chebulic acid with 7LVW

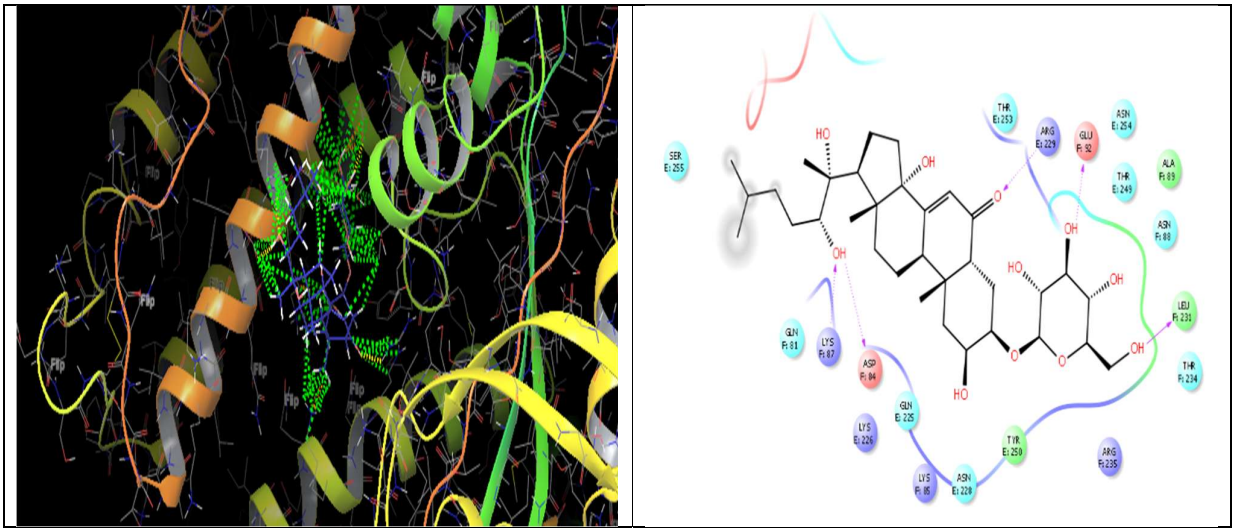

Figure 5: Interaction of Hesperidin with 7LVW

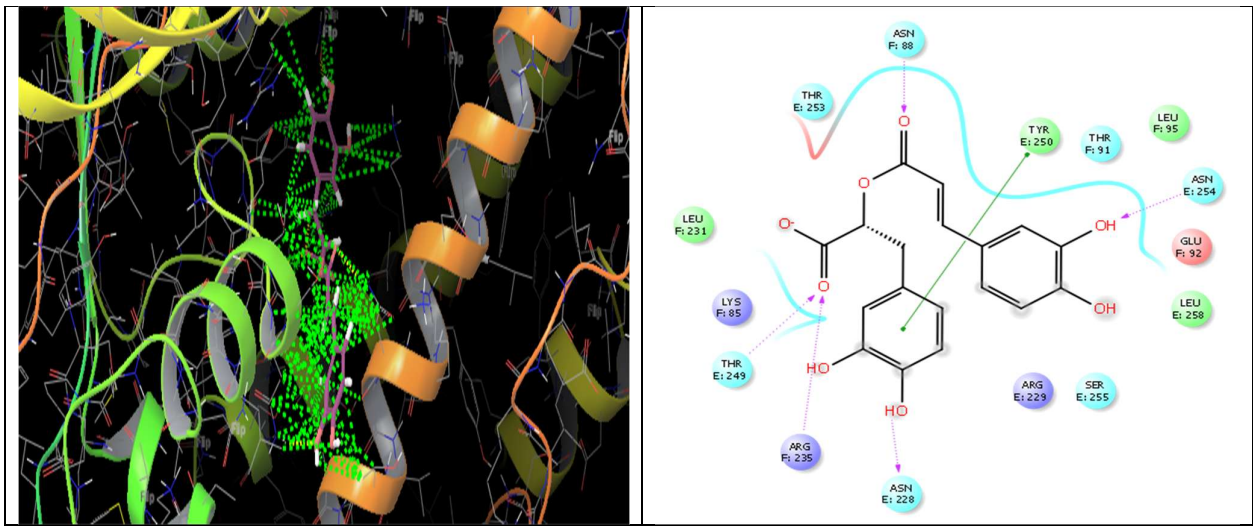

Figure 6: Interaction of Rosamarinic Acid with 7LVW

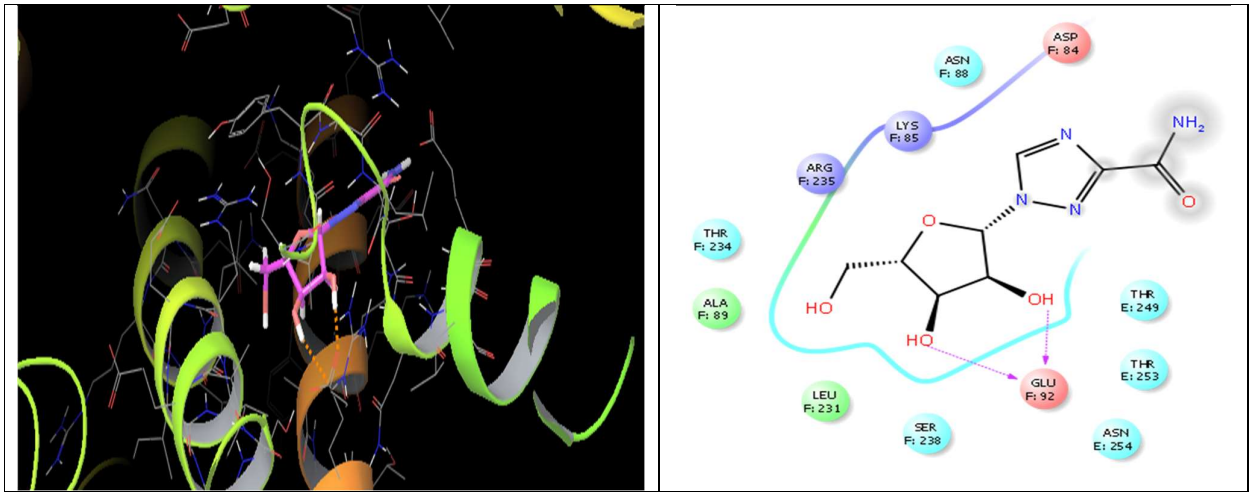

Figure 7: Interaction of Ribavirin (standard) with 7LVW

B. **Determination of ADME/Tox for lead compounds**

ADMET2.0 was employed to evaluate the physicochemical parameters essential for drug candidates, including their toxicological properties. According to the Lipinski Rule of Five, a compound is considered drug-like if it does not exceed more than one of the following criteria: a molecular weight greater than 500 Da, an octanol-water partition coefficient (LogP) less than 5, no more than 5 hydrogen bond donors, and no more than 10 hydrogen bond acceptors. The physicochemical parameters for the compounds were calculated using ADMET2.0 to ensure they meet these criteria, thus assessing their potential as viable drug candidates **[12]**.

Table 3: Physicochemical Properties of lead Compounds [13]

Ligands	Molecular Weight	Density	Number Of Hydrogen Bond Donor	Number Of Hydrogen Bond Acceptor	Log S	Log P	Log D
Chebulagic Acid	954.100	1.141	13	27	-3.57	1.220	1.515
Chebulic Acid	956.110	1.131	13	27	-3.084	1.436	0.959
Eugenin	206.060	1.021	1	4	-2.493	2.350	2.053
Gaultherin	446.140	1.098	6	12	-1.653	-0.431	-0.617
Hesperidin	610.19	1.083	8	15	-3.504	-0.59	1.156
Punarnavoside	626.37	0.997	8	11	-2.916	1.635	1.713
Quercetin	302.4	1.068	5	7	-3.671	2.155	1.767
Rosamarinic Acid	360.080	1.031	5	8	-2.432	1.775	1.650
Sisunatovir(Std)	446.170	1.063	2	5	-3.055	3.023	2.750
Ribavirin(Std)	244.080	1.163	5	9	-0.310	-2.006	-1.633

Table 4: Medicinal Chemistry of lead Compounds [14]

Ligand	Lipinski rule	GSK rule	Pfizer rule	QED
Chebulagic acid	Rejected	Rejected	Accepted	0.055
Chebulic acid	Rejected	Rejected	Accepted	0.045
Eugenin	Accepted	Accepted	Accepted	0.773
Gaultherin	Rejected	Rejected	Accepted	0.246
Hesperidin	Rejected	Rejected	Accepted	0.185
Punarnavoside	Rejected	Rejected	Accepted	0.187
Quercetin	Accepted	Accepted	Accepted	0.434
Rosamarinic acid	Accepted	Accepted	Accepted	0.298
Sisunatovir(std)	Accepted	Rejected	Rejected	0.565
Ribavirin(std)	Accepted	Accepted	Accepted	0.443

Table 5: Absorption parameters of Lead Compounds [15]

Ligand	Caco2 Permeability	MDCK Permeability	Bioavailability
Chebulagic Acid	-7.001	1.40E-5	1
Chebulic Acid	-7.13	2.23E-05	1
Eugenin	-4.771	1.4E-05	0.978
Gaultherin	-6.317	6.11E-05	0.993
Hesperidin	-6.484	9.40E-05	0.999
Punarnavoside	-5.074	0.000156	0.712
Quercetin	-5.204	8E-06	0.997
Rosamarinic Acid	-6.005	6.9E-06	0.994
Sisunatovir(Std)	-5.105	1.2e-05	0.003
Ribavirin(Std)	-5.582	0.00024	0.155

Table 6: Distribution Parameters of Lead Compounds [16]

Ligand	Plasma Protein Binding	Volume Of Distribution	BBB Penetration
Chebulagic Acid	85.45%	0.479	0
Chebulic Acid	81.64%	0.419	0.012
Eugenin	83.95%	0.833	0.007
Gaultherin	28.25%	0.56	0.198
Hesperidin	77.64%	0.935	0.254
Punarnavoside	79.98%	0.7	0.13
Quercetin	95.49%	0.579	0.008
Rosamarinic Acid	97.72%	0.369	0.049
Sisunatovir(Std)	72.44%	2.587	0.915
Ribavirin(Std)	7.891%	0.875	0.646

Table 7: Excretion Parameters of Lead Compounds [17]

Ligand	Clearance	T1/2
Chebulagic Acid	6.866	0.969
Chebulic Acid	9.336	0.982
Eugenin	6.124	0.635
Gaultherin	1.053	0.788
Hesperidin	1.489	0.195
Punarnavoside	1.319	0.087
Quercetin	8.284	0.929
Rosamarinic Acid	15.347	0.959
Sisunatovir(Std)	5.081	0.127
Ribavirin(Std)	4.138	0.530

Table 8: Toxicity Parameters of Lead Compounds

Ligand	Skin Sensitization	AMES Toxicity	Carcinogenicity
Chebulagic Acid	0.706	0.045	0.01
Chebulic Acid	0.939	0.044	0.009
Eugenin	0.632	0.564	0.048
Gaultherin	0.376	0.185	0.055
Hesperidin	0.03	0.499	0.87
Punarnavoside	0.019	0.128	0.037
Quercetin	0.919	0.657	0.05
Rosamarinic Acid	0.951	0.035	0.275
Sisunatovir(Std)	0.247	0.82	0.803
Ribavirin(Std)	0.023	0.039	0.124

RESULT AND DISCUSSION

The comprehensive docking analysis of the 7LVW protein with various ligands revealed significant interactions and binding affinities, providing valuable insights into potential therapeutic candidates. A highly favorable site map was generated with a score of -1.39, which guided the subsequent grid creation and detailed molecular docking studies. The findings from these studies indicated that Chebulic Acid (-6.27), Hesperidin (-5.57), and Rosmarinic Acid (-6.57) demonstrated superior docking scores compared to the standard drugs Ribavirin and Sisunatovir, suggesting these natural compounds may offer enhanced binding affinity and interaction with the target protein. In addition to the docking studies, an ADMET analysis was performed using the ADMET 2.0 software to evaluate the pharmacokinetic and toxicity profiles of these promising ligands. The results from this ADMET study highlighted that Chebulic Acid, Hesperidin, and Rosmarinic Acid possess high potential as therapeutic agents. These compounds exhibited favorable properties such as optimal LogP (partition coefficient), LogD (distribution coefficient), and bioavailability, indicating their efficient absorption and distribution within the body. Moreover, they demonstrated effective blood-brain barrier (BBB) penetration, suggesting potential central nervous system activity. The half-lives of these compounds were also favorable, indicating their sustained presence in the system. Importantly, these ligands showed minimal toxicity, underscoring their safety profile as potential drug candidates. Overall,

the combination of high docking scores and promising ADMET properties positions Chebulic Acid, Hesperidin, and Rosmarinic Acid as strong candidates for further development in therapeutic applications.

CONCLUSION

In the molecular docking studies and ADME/tox evaluations conducted on 50 natural compounds from the IBS database have identified several promising antiviral agents against RSV. The comprehensive analysis revealed that Chebulic Acid, Hesperidin, and Rosmarinic Acid stand out as highly effective candidates, demonstrating superior docking scores, favorable glide energy, and excellent ADME/tox profiles. These compounds showed greater inhibitory potential against the 7LVW protein of RSV compared to traditional synthetic drugs such as Ribavirin and Sisunatovir. This study underscores the utility of in-silico molecular docking and ADMET analysis in identifying and evaluating novel antiviral agents, paving the way for further research and development in the quest for effective RSV treatments. The findings suggest that these natural compounds could play a significant role in future antiviral drug discovery and development.

ACKNOWLEDGMENT

The authors wish to express their gratitude to all the co-authors for their valuable guidance and support.

REFERENCES

[1] Edward E Walish and Caroline Breese Hall, Respiratory Syncytial Virus, National Library of Medicine,18 (2014). https://doi.org/10.1016%2FB978-1-4557-4801-3.00160-0

[2] Anusha Hindpur, Thangam Menon, Epidemology of Respiratory Syncytial Virus Infections in Chennai, South Africa, Volume 3, Issue 3, P-288-299, (2019).

[3] Tatyana M Khomenko, Anna A Shtro, Monoterpene-Containing Substituted Coumarins as Inhibitors of RSV Replication, Molecules ,26, 7493, (2023).

[4] Lakshmi Narayan venu, Antiviral efficacy of medicinal plants against respiratory viruses: Respiratory Syncytial virus (RSV) and coronavirus (CoV)/ Covid 19, The Journal of Phytopharmacolgy, 9(4): 281-290, (2009).

[5] Lea eiland, Respiratory Syncytial virus: Diagnosis treatment and prevention, The Journal of pediatric pharmacology and therapeutics, Vol.14, 75-85, (2019).

[6] Olusola Olalekan elekofehiniti, Molecular Docking studies, molecular dynamics and ADME/tox reveal therapeutics potential of STOCKIN-69160 aganist papain like of protease of SARS-Cov-2, Springer, ,25: 1761-1773,(2020).

[7] Emmanuel oluwaseum Adediran, Repurposing Antidiabetic Drugs Against Respiratory Syncytial Viral Infection: A Docking Study, Computational Molecular Bioscience, Jun 13,(2022). https://doi.org/10.4236/cmb.2022.122005

[8] Michela Cancelleri, In Silico Structure Based Design and Synthesis of Novel Anti-RSV compounds, Elsevier, 46-50,(2015). https://doi.org/10.1016/j.antiviral.2015.08.003

[9] Khalid Alshaghdali, Identification of Respiratory Syncytial Virus Fusion Protein Inhibitor: In silico Screening and Molecular Docking approach, Journal of Pharmaceutical Research International,41-48,(2018).

[10] https://pubchem.ncbi.nlm.nih.gov

[11] https://newsite.schrodinger.com/platform/products/maestro/

[12] https://admetmesh.scbdd.com/

[13] Y Inaba, Physicochemical Properties of Bovine Respiratory Syncytial Virus, National Library of Medicine,6-8,(2018).

[14] Lu Mao, Design, Synthesis and Anti-Respiratory Syncytial virus potential of novel 3-(1,2,3-triazol-1-yl) furoxazine -fused benzimidazole derivatives,7-10,(2023).

[15] Battles Michael B, Molecular Mechanisms of Respiratory Syncytial Virus Fusion Inhibitors, Nature Chemical Biology, 87-93,(2015).

[16] Yassine, Hadi M, Systematic Review of the Respiratory Syncytial Virus (RSV) Prevalence, Genotype distribution and seasonality in Children from the middle East and Northern, microorganisms,5-8, (2020). https://doi.org/10.3390%2Fmicroorganisms8050713

[17] Sun -Bo-wen, Prevention of Potential Treatment Strategies for Respiratory Syncytial Virus, Molecule, 598, (2024).